Comparative neutronic analysis of solid and annular (Th-^{233}U-^{235}U)O_2 fuel assemblies with variable H_2O/D_2O moderator compositions

HANAN RIFAI[1], OUADIE KABACH[*, 2], FADI EL BANNI[3], HAMID AMSIL[4], EL MAHJOUB CHAKIR[2], ZOUHAIR SADOUNE[1]

[1]Laboratory of Electronic Systems, Information Processing, Mechanics and Energy, Faculty of Sciences, Ibn Tofail University, Kenitra, Morocco.

[2]Laboratory of Materials and Subatomic Physics, Faculty of Sciences, Ibn Tofail University, Kenitra, Morocco

[3]Institute for Research on New Energies, Nangui Abrogoua University, Abidjan, Ivory Coast

[4] National Center for Energy, Sciences and Nuclear Technique, Rabat, Morocco

[*] Corresponding authors: hrifai4@gmail.com (Hanan Rifai); ouadie.kabach10@gmail.com (Ouadie Kabach)

Abstract

This study investigates the neutronic performance of mixed H_2O/D_2O moderated reactor assemblies utilizing an innovative (Th-^{233}U-^{235}U)O_2 ternary fuel composition in both solid and dual-cooled annular configurations within the AP300™ small modular reactor. Twenty-three configurations were systematically analyzed using the DRAGON deterministic lattice physics code, with deuterium concentrations varying from 0% to 100% in 10% increments, to comprehensively characterize the effects of moderator composition on reactor physics parameters.

The results demonstrate optimal neutronic performance within the 0-30% D_2O range, where both configurations achieve remarkable fuel cycle extensions of 20-25% compared to conventional UO_2 fuel. The solid configuration with pure H_2O moderation achieves 170.800 GWd/t discharge burnup and 821.548 EFPDs cycle length, while the annular design reaches 166.306 GWd/t and 799.932 EFPDs. Progressive deuterium enrichment beyond 30% leads to systematic performance degradation due to spectral hardening effects that disrupt the thorium breeding cycle, with configurations exceeding 80% D_2O failing to maintain adequate criticality. Reactivity coefficient analysis exposes critical safety implications, with fuel temperature coefficients becoming increasingly negative (beneficial) while moderator temperature coefficients transition from negative to positive values (concerning) with rising D_2O content.

Keywords: *Small modular reactor (SMR); Thorium fuel cycle; Mixed moderator; Dual-cooled annular fuel; Reactivity coefficients.*

1. Introduction

The landscape of SMR technology continues to evolve beyond traditional paradigms, with contemporary designs predominantly relying on established light water reactor (LWR) principles. These systems conventionally employ UO_2 fuel, fabricated as solid cylindrical pellets, which are hermetically sealed within zirconium-based alloy cladding and arranged in a square lattice arrangement. While this configuration has proven its reliability through extensive commercial deployment, the pursuit of enhanced thermal performance and safety margins has catalyzed the development of innovative fuel geometries that challenge these conventional approaches [1–3].

Among the most compelling advances in fuel design is the dual-cooled annular configuration, which fundamentally reimagines the heat transfer paradigm through its distinctive hollow cylindrical architecture [4–9]. This geometry, as illustrated in Fig. 1, facilitates coolant circulation along both the interior and exterior surfaces of the fuel element, achieving a transformative enhancement in thermal management capabilities. The annular design delivers two critical improvements that directly enable higher power density operation. The shortened thermal conduction pathway from the fuel material to the cooling surfaces maintains substantially larger margins between operating temperatures and fuel melting limits, thereby strengthening inherent safety characteristics. Additionally, despite accommodating fewer individual fuel elements per assembly, the dramatically expanded heat transfer surface area delivers superior thermal removal capacity and provides enhanced protection against departure from nucleate boiling phenomena [4,5,9–16].

The strategic selection of fuel composition represents another crucial dimension in optimizing reactor performance characteristics. Our recent investigations have introduced an innovative ternary oxide system, designated as (Th-^{233}U-^{235}U)O_2, which presents compelling advantages relative to both conventional uranium dioxide and binary thorium-uranium compositions, including (Th-^{235}U)O_2 and (Th-^{233}U)O_2 configurations [17–25]. This advanced fuel formulation synergistically combines Th-232 with dual fissile isotopes, U-233 and U-235, thereby exploiting their complementary nuclear properties. The practical implementation of this fuel system leverages existing nuclear infrastructure, with U-235 recoverable from reprocessed spent fuel inventories where it persists at concentrations of approximately 0.5 to 1.0 wt.%, corresponding to roughly 5-10 kilograms per metric ton of original uranium. The U-233 component can be produced through controlled irradiation of thorium targets, followed by appropriate cooling intervals and chemical separation processes [26].

This ternary fuel formulation demonstrates multiple performance advantages that enhance reactor operations. The incorporation of Th-232 strengthens the negative fuel temperature coefficient through enhanced Doppler broadening mechanisms, providing robust inherent safety feedback during temperature transients. Furthermore, the system exhibits more favorable moderator temperature coefficient characteristics compared to binary (Th-^{233}U)O_2 compositions, contributing to improved reactor stability and control response. The fuel composition also demonstrates superior neutron economy, achieving criticality with reduced fissile inventory requirements relative to a pure (Th-^{233}U)O_2 reactor, thereby optimizing resource utilization [17–25].

The moderation of neutrons represents a fundamental process in thermal reactor physics, particularly given that the overwhelming majority of commercial power reactors utilize water in the dual capacity of neutron moderator and heat removal medium [27,28]. Neutrons liberated through fission events possess substantial kinetic energies, typically centered around 2 MeV. In contrast, the probability of inducing subsequent fissions increases dramatically at thermal energies due to the significantly larger thermal fission cross-sections. Effective moderation, therefore, requires the systematic reduction of neutron energies through repeated elastic scattering interactions with light nuclei. Table 1 presents the key nuclear properties of

common reactor moderators. In contrast, Table 2 illustrates the varying number of collisions required for different moderating materials to thermalize fast neutrons from 2 MeV to thermal energies of 0.025 eV.

The effectiveness of moderation processes can be characterized through several fundamental parameters. The slowing-down power, defined as the product of the average logarithmic energy decrement per collision and the macroscopic scattering cross-section, quantifies the rate of neutron energy reduction within the moderating medium. However, a more comprehensive assessment of moderator performance requires consideration of the moderating ratio, calculated as the slowing-down power divided by the macroscopic absorption cross-section. This metric accounts for both the efficiency of energy reduction and the probability of neutron preservation during the moderation process. As shown in Table 1, while ordinary water exhibits superior slowing-down power, heavy water demonstrates an exceptional moderating ratio of 4150 compared to 68 for light water, attributable to deuterium's remarkably low neutron absorption probability of only 0.0013 barns versus 0.66 barns for hydrogen [27–29].

These contrasting moderator characteristics suggest that strategically blending light and heavy water could optimize neutron spectral properties while balancing economic considerations. Mixed H_2O/D_2O systems offer the potential to combine the rapid thermalization characteristics of ordinary water with the superior neutron economy afforded by heavy water's minimal parasitic absorption. Through systematic variation of the deuterium concentration, the neutron energy distribution can be precisely tailored to maximize the performance of advanced fuel systems, particularly those incorporating thorium-based compositions. This spectral optimization capability becomes increasingly valuable when integrated with innovative fuel geometries that inherently enhance neutron utilization efficiency [28–30].

Fig. 1. Cross-sectional comparison of solid and annular fuel rod configurations (not to scale) [7].

Building upon the theoretical advantages of mixed moderation discussed above, the present investigation explores the synergistic effects of combining H_2O/D_2O moderator with advanced fuel designs. Specifically, this work systematically examines how varying ratios of light and heavy water moderation influence the neutronic behavior of the innovative (Th-^{233}U-^{235}U)O_2 fuel when deployed in both conventional solid and dual-cooled annular rod configurations within the operational framework of the AP300^{TM} SMR design.

The comprehensive analysis encompasses the influence of D_2O wt.% ranging from pure H_2O to pure D_2O on critical operational parameters, including cycle length extension, achievable discharge burnup, fuel depletion characteristics, and the evolution of key reactivity coefficients, specifically the fuel and moderator temperature coefficients that govern reactor stability and safety response. Performance metrics are benchmarked against the reference

configuration employing standard UO_2 fuel in solid geometry with conventional H_2O moderation, providing a quantitative assessment of the potential benefits achievable through the strategic combination of advanced fuel compositions, innovative geometries, and optimized mixed moderator systems.

Table 1. Common reactor moderators [31].

Compound	Neutron scattering cross section (barns)	Neutron absorption cross section (barns)	Moderating ratio
Light water H_2O	49	0.66	68
Heavy water D_2O	10.6	0.0013	4150
Graphite (C)	4.7	0.0035	212

Table 2. Average number of collisions needed to thermalize a high-energy neutron (2 MeV to 0.025 eV) [31].

Element	Atomic weight	Number of collisions
Water	18	20
Hydrogen	1	27
Deuterium	2	31
Heavy water	20	36
Helium	4	48
Beryllium	9	92
Carbon	12	119

2. Model design and input parameters

2.1. Description of the SMR case used for the investigation

The neutronic analysis presented in this study utilizes the Westinghouse AP300™ SMR as the computational framework and reference configuration. This advanced reactor system, classified as Generation III+ technology and developed by Westinghouse Electric Company, generates an electrical output of 330 MWe through conversion of 990 MWt thermal power. The design approach leverages the operational experience and regulatory approval pathway established by the larger AP1000® platform, employing a systematic scaling methodology that preserves the fundamental safety features and operational characteristics while adapting them to the smaller thermal capacity. The reactor core architecture employs a conventional PWR layout comprising 121 fuel assemblies. Each assembly maintains the standard Westinghouse 17×17 lattice structure, incorporating 264 active fuel positions per assembly alongside dedicated locations for control rod guide tubes and instrumentation thimbles. Under baseline operating conditions, the core is planned to utilize conventional UO_2 fuel pellets with enrichment levels maintained below 5 wt.%. The fuel management strategy nominally targets 36-month operational cycles between refueling outages, though the core design incorporates sufficient flexibility to accommodate extended cycles up to 48 months through appropriate adjustments to initial enrichment and burnable absorber loadings [32–36].

2.2. Specification of the reference assembly and proposed models

This investigation evaluates two assembly configurations: a reference case using conventional solid UO_2 fuel in a 17×17 array, and an advanced design employing (Th-^{233}U-^{235}U)O_2 fuel in both solid and dual-cooled annular geometries. Fig. 2 presents the models for both configurations, showing the distinction between solid cylindrical and annular fuel elements with internal/external cooling channels. Table 3 details the fuel specifications:

standard UO_2 and (Th-^{233}U-^{235}U)O_2. The geometric parameters in Table 4 show that while both assemblies maintain a 21.5 cm pitch, the solid configuration contains 264 rods in a 17 × 17 lattice, whereas the annular design accommodates 160 rods in a 13 × 13 array with a larger rod pitch (1.65 cm vs. 1.26 cm) to accommodate the dual-cooling channels. The parametric study, summarized in Table 5, comprises 23 cases: one reference (UO_2 with H_2O) and 22 cases examining (Th-^{233}U-^{235}U)O_2 fuel in solid (So_case1-11) and annular (DC_case1-11) configurations with D_2O concentrations varying from 0% to 100% in 10% increments. This systematic approach aims to comprehensively characterize the effects of mixed moderators on reactor physics parameters and fuel performance.

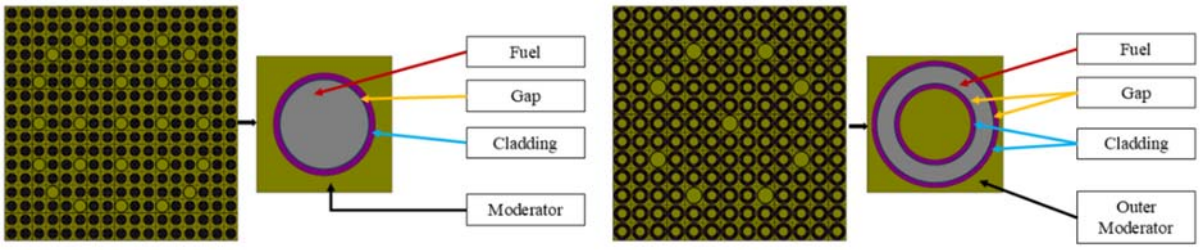

Fig. 2. Computational modeling of solid and annular assembly configurations and fuel elements via DRAGON code.

Table 3. Properties of the analyzed fuel type [25,37,38].

Fuel	Density (g/cm^3)	Fissile enrichment (wt.%)
UO_2	10.412 (95% of TD)	4.95 % (U-235)
(Th-^{233}U-^{235}U)O_2	9.50 (95% of TD)	2.475 % (U-233) + 2.475 % (U-235)

Table 4. Assembly-level parameters considered in the simulations.

Parameter	Solid assemblies	Annular assemblies
Rod array	17 × 17	13 × 13
Number of fuel rods	264	160
Number of guide tubes	24	9
Assembly pitch (cm)	21.5	21.5
Rod lattice pitch (cm)	1.26	1.65
Inner clad inner radius (cm)	-	0.43165
Inner clad outer radius (cm)	-	0.48885
Inner gap outer radius (cm)	-	0.49705
Fuel outer radius (cm)	0.40960	0.70644
Outer gap outer radius (cm)	0.41780	0.71464
Outer clad outer radius (cm)	0.47500	0.77184
Guide tube inner radius (cm)	0.56	0.71
Guide tube outer radius (cm)	0.60	0.77

Table 5. Description of the assembly cases investigated in the study with corresponding IDs.

Case Name	Description	Case Name	Description
Reference case	Solid (17 × 17) with UO_2 fuel	-	-
So_case1	Solid (17 × 17) with (Th-^{233}U-^{235}U)O_2 fuel. The moderator is H_2O.	DC_case1	Dual-cooled (13 × 13) with (Th-^{233}U-^{235}U)O_2 fuel. The moderator is H_2O.
So_case2	Solid (17 × 17) with (Th-^{233}U-^{235}U)O_2 fuel. The moderator is 90%H_2O/10%D_2O.	DC_case2	Dual-cooled (13 × 13) with (Th-^{233}U-^{235}U)O_2 fuel. The moderator is 90%H_2O/10%D_2O.

So_case3	Solid (17 × 17) with (Th-^{233}U-^{235}U)O_2 fuel. The moderator is 80%H_2O/20%D_2O.	DC_case3	Dual-cooled (13 × 13) with (Th-^{233}U-^{235}U)O_2 fuel. The moderator is 80%H_2O/20%D_2O.
So_case4	Solid (17 × 17) with (Th-^{233}U-^{235}U)O_2 fuel. The moderator is 70%H_2O/30%D_2O.	DC_case4	Dual-cooled (13 × 13) with (Th-^{233}U-^{235}U)O_2 fuel. The moderator is 70%H_2O/30%D_2O.
So_case5	Solid (17 × 17) with (Th-^{233}U-^{235}U)O_2 fuel. The moderator is 60%H_2O/40%D_2O.	DC_case5	Dual-cooled (13 × 13) with (Th-^{233}U-^{235}U)O_2 fuel. The moderator is 60%H_2O/40%D_2O.
So_case6	Solid (17 × 17) with (Th-^{233}U-^{235}U)O_2 fuel. The moderator is 50%H_2O/50%D_2O.	DC_case6	Dual-cooled (13 × 13) with (Th-^{233}U-^{235}U)O_2 fuel. The moderator is 50%H_2O/50%D_2O.
So_case7	Solid (17 × 17) with (Th-^{233}U-^{235}U)O_2 fuel. The moderator is 40%H_2O/60%D_2O.	DC_case7	Dual-cooled (13 × 13) with (Th-^{233}U-^{235}U)O_2 fuel. The moderator is 40%H_2O/60%D_2O.
So_case8	Solid (17 × 17) with (Th-^{233}U-^{235}U)O_2 fuel. The moderator is 30%H_2O/70%D_2O.	DC_case8	Dual-cooled (13 × 13) with (Th-^{233}U-^{235}U)O_2 fuel. The moderator is 30%H_2O/70%D_2O.
So_case9	Solid (17 × 17) with (Th-^{233}U-^{235}U)O_2 fuel. The moderator is 20%H_2O/80%D_2O.	DC_case9	Dual-cooled (13 × 13) with (Th-^{233}U-^{235}U)O_2 fuel. The moderator is 20%H_2O/80%D_2O.
So_case10	Solid (17 × 17) with (Th-^{233}U-^{235}U)O_2 fuel. The moderator is 10%H_2O/90%D_2O.	DC_case10	Dual-cooled (13 × 13) with (Th-^{233}U-^{235}U)O_2 fuel. The moderator is 10%H_2O/90%D_2O.
So_case11	Solid (17 × 17) with (Th-^{233}U-^{235}U)O_2 fuel. The moderator is 100%D_2O.	DC_case11	Dual-cooled (13 × 13) with (Th-^{233}U-^{235}U)O_2 fuel. The moderator is 100%D_2O.

2.3. Calculation procedures for neutronic analysis

The neutronic calculations were performed using DRAGON, a deterministic lattice physics code developed by École Polytechnique de Montréal for reactor physics analysis. Fig. 2 depicts the two-dimensional models designed for both solid and annular assembly configurations. The simulation workflow combined several DRAGON modules: GEO for geometry definition, EXCELT for spatial discretization, MCCGT for transport solutions using Suslov's long characteristics technique, and SHI for resonant self-shielding. Nuclear data processing made use of the ENDFB-VIII.0 library with SHEM-361 energy group structure. Depletion calculations were carried out using the EVO module, and spatial homogenization was accomplished using EDI [17,18,43,19–21,25,39–42].

Assembly performance evaluation employed the Linear Reactivity Model (LRM), which exploits the approximately linear relationship between reactivity and burnup in PWR systems [44,45] . Core reactivity is expressed as:

$$\rho = \frac{k_{inf} - (1 + L)}{k_{inf}} \quad (1)$$

where ρ denotes reactivity, k_{inf} represents the infinite multiplication factor, and L accounts for neutron leakage. For SMR applications, a 7% leakage correction was applied, reflecting the higher neutron escape probability in compact cores compared to conventional PWRs (~3%). Discharge burnup was therefore determined when k_{inf} reached 1.07 [12,46].

Multi-batch fuel management calculations utilized the following relationships:

$$B_{Discharge} = \frac{2N_{NB}}{(N_{NB} + 1)} B_{SB} \quad (2)$$

$$T_{cycle} = \frac{2}{(N_{NB} + 1)} \frac{B_{SB}}{P_{SPD}} \quad (3)$$

where N_{NB} denotes the number of batches, B_{SB} represents single-batch burnup, T_{cycle} denotes cycle length expressed in effective full power days (EFPDs), and P_{SPD} is the specific power density. For a three-batch operation, discharge burnup increases by a factor of 1.5 relative to single-batch values.

Reactor safety characteristics were assessed through fuel and moderator temperature coefficients [24,42]. The FTC quantifies Doppler feedback effects through:

$$FTC = \frac{k_{inf}(T) - k_{inf,0}}{k_{inf,0}\Delta T} \quad (4)$$

where $k_{inf}(T)$ represents the multiplication eigenvalue at the perturbed fuel temperature, $K_{inf,0}$ denotes the eigenvalue under nominal operating conditions, and ΔT fuel is the applied temperature perturbation.

For this analysis, a temperature increment of 100 K was selected to ensure sufficient sensitivity while maintaining computational accuracy within the linear response regime. The MTC calculation incorporated coupled temperature-density effects to accurately represent coolant thermodynamic states

$$MTC = \frac{k_{inf}(T, \rho) - k_{inf,0}}{k_{inf,0}\Delta T} \quad (6)$$

where $K_{inf}(T, \rho)$ is calculated with concurrent moderator temperature and density variations corresponding to the thermodynamic state at the perturbed condition. A temperature perturbation of 20 K was applied for the MTC calculations [17].

3. Results

3.1. Fuel burnup

Fig. 3 illustrates the evolution of k_{inf} as a function of burnup for all 23 investigated configurations, revealing distinct behavioral patterns that correlate strongly with moderator composition and fuel geometry. The reference UO_2 assembly exhibits a quasi-linear decrease from an initial k_{inf} of 1.398396 to 0.968177 at 31.65 GWd/t, where it intersects the critical threshold of 1.07, accounting for 7% neutron leakage in the compact SMR core. This baseline performance establishes the benchmark against which the advanced ternary fuel configurations are evaluated.

The (Th-^{233}U-^{235}U)O_2 fuel configurations demonstrate markedly different depletion characteristics depending on D_2O concentration, with three distinct performance regimes emerging from the data. In the optimal performance regime spanning 0-30% D_2O, both solid and annular configurations maintain high initial k_{inf} values ranging from 1.40 to 1.43 with gradual depletion rates. The solid geometry cases show exceptional performance, with So_case1 utilizing pure H_2O exhibiting a BOC k_{inf} of 1.43354, the highest among all solid cases, followed by So_case2 with 10% D_2O at 1.42387 and So_case3 with 20% D_2O at 1.41157. The annular configurations demonstrate similar but slightly lower initial

multiplication factors, with DC_case1 showing 1.40666 for pure H_2O, DC_case2 achieving 1.39614 at 10% D_2O, and DC_case3 reaching 1.38307 at 20% D_2O. This consistent 2-3% lower k_{inf} in annular designs reflects their reduced fuel inventory and different neutron flux distribution patterns. Both geometries maintain relatively flat depletion curves in this optimal regime, declining at approximately 0.008-0.009 per GWd/t for solid cases and 0.009-0.010 per GWd/t for annular cases. The superior performance with pure light water moderation in both configurations stems from enhanced thorium utilization and balanced fissile depletion in the thermal neutron spectrum, where effective breeding of U-233 from the thorium matrix through Pa-233 decay compensates for fissile consumption, maintaining higher reactivity levels throughout the cycle.

As D_2O concentration increases into the transitional regime of 40-70%, progressive degradation in neutronic performance becomes evident for both configurations. Initial k_{inf} values decrease systematically in solid cases from 1.39597 for So_case4 with 30% D_2O to 1.37583 for So_case5 with 40% D_2O, further declining to 1.34972 for So_case6 at 50% D_2O, 1.31543 for So_case7 at 60% D_2O, and reaching 1.26809 for So_case8 at 70% D_2O. The annular configurations exhibit parallel degradation patterns with DC_case4 at 30% D_2O showing 1.36669, DC_case5 at 40% D_2O reaching 1.34593, DC_case6 at 50% D_2O declining to 1.31919, DC_case7 at 60% D_2O dropping to 1.28399, and DC_case8 at 70% D_2O falling to 1.23619. The steeper depletion slopes with annular cases show depletion rates of 0.011-0.013 per GWd/t compared to 0.010-0.012 per GWd/t for solid cases. This accelerated reactivity loss is attributed to the hardening neutron spectrum that shifts the fission-to-capture ratio unfavorably for the U-233/U-235 system, with the effect being more pronounced in annular geometry due to the altered neutron leakage patterns.

In the subcritical regime with 80-100% D_2O, both solid and annular cases exhibit severely compromised performance. So_case9 at 80% D_2O manages initial criticality with k_{inf} of 1.20042 but rapidly depletes, while DC_case9 shows 1.16821, already marginal for sustained operation. The situation deteriorates dramatically at higher D_2O concentrations, with So_case10 at 90% D_2O achieving only 1.09727 at BOC, barely above the critical threshold, while DC_case10 shows 1.06514, failing to provide adequate excess reactivity for practical operation. The pure D_2O cases demonstrate complete incompatibility with the fuel design, as So_case11 shows a k_{inf} of only 0.92389 at BOC while DC_case11 reaches merely 0.89219, both falling significantly below the critical threshold of 1.07. The annular configurations consistently show 3-4% lower k_{inf} values than their solid counterparts in this regime, confirming that the harder spectrum in heavy water fundamentally disrupts the fuel's neutronic balance in both geometries, with the effect being more severe in the reduced-inventory annular design. Table 6 quantifies the single-batch discharge burnup achievements across all configurations, revealing systematic performance differences between geometries.

Table 7 presents the three-batch fuel management performance. The results reveal remarkable burnup extensions for optimally moderated cases in both geometries. So_case1 using pure H_2O achieves 170.800 GWd/t discharge burnup and 821.548 EFPD cycle length, while DC_case1 with pure H_2O attains 166.306 GWd/t and 799.932 EFPDs. With 10% D_2O addition, So_case2 reaches 169.410 GWd/t and 814.863 EFPDs, whereas DC_case2 achieves 164.121 GWd/t and 789.422 EFPDs. At 20% D_2O, So_case3 maintains 167.013 GWd/t with 803.332 EFPDs, while DC_case3 reaches 160.714 GWd/t with 773.036 EFPDs. These values represent 20-25% improvements in both burnup and cycle length compared to the reference UO_2 case at 142.438 GWd/t with 685.127 EFPDs. The extended cycles with pure H_2O moderation in both geometries approach the targeted 36-month refueling interval of approximately 800 EFPDs at 75% capacity factor, with solid configurations exceeding this target while annular designs fall just short.

The burnup capability exhibits increasingly severe degradation as D_2O concentration rises above 30% in both configurations. From peak performance with pure H_2O, minimal degradation of less than 2% occurs at 10-20% D_2O for both geometries. At 40% D_2O, So_case5 discharge burnup decreases to 157.084 GWd/t, representing an 8% reduction from peak, while DC_case5 drops to 147.740 GWd/t for an 11% reduction. At 60% D_2O, So_case7 yields 132.365 GWd/t for a 23% reduction, whereas DC_case7 achieves only 117.802 GWd/t, showing a 29% reduction. The degradation becomes severe at 80% D_2O, where So_case9 falls to 65.172 GWd/t, representing a 62% reduction, while DC_case9 manages only 41.423 GWd/t for a 75% reduction from peak performance. Configurations with 90% or higher D_2O cannot sustain criticality throughout even a single batch in either geometry, with annular cases failing earlier in the cycle than solid configurations.

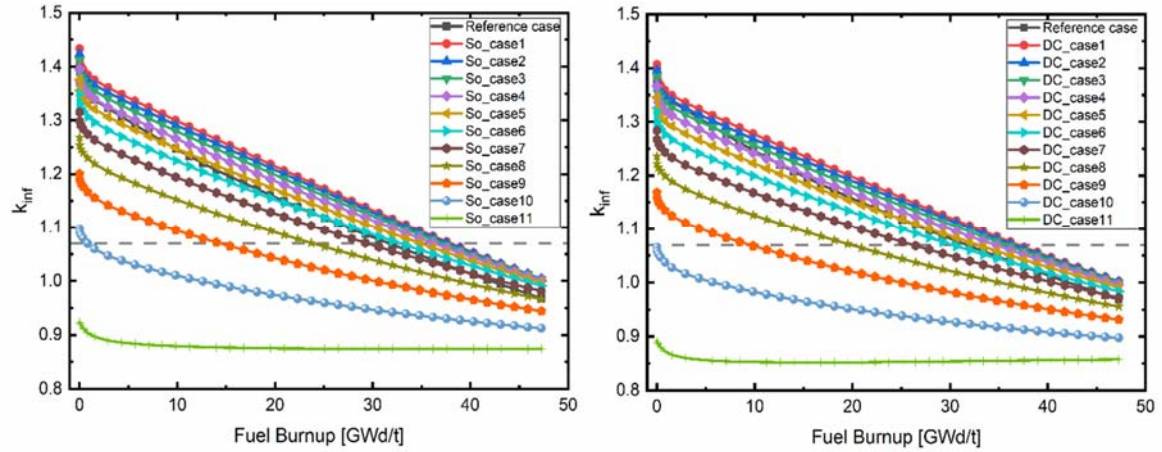

Fig. 3. Burnup-dependent k_{inf} for the investigated solid and dual-cooled annular cases.

Table 6. k_{inf} at BOC and EOC and Single-batch discharge burnup (B_{SB}) for (a) solid cases, (b) dual-cooled annular cases.

(a)

Cases	k_{inf} (BOC)	k_{inf} (EOC)	B_{SB} (GWd/t)
Reference case	1.398396	0.968177	31.653
So_case1	1.433537	1.003852	37.956
So_case2	1.423868	1.004158	37.647
So_case3	1.411571	1.003478	37.114
So_case4	1.395965	1.001455	36.256
So_case5	1.375833	0.997621	34.907
So_case6	1.349721	0.991324	32.791
So_case7	1.315429	0.981514	29.414
So_case8	1.268088	0.966526	23.862
So_case9	1.200420	0.944263	14.483
So_case10	1.097260	0.912404	0.857
So_case11	0.923886	0.874625	0.000

(b)

Cases	k_{inf} (BOC)	k_{inf} (EOC)	B_{SB} (GWd/t)
Reference case	1.398396	0.968177	31.653
DC_case1	1.406659	1.001783	36.957
DC_case2	1.396140	1.001242	36.471
DC_case3	1.383071	0.999583	35.714

DC_case4	1.366694	0.996474	35.714
DC_case5	1.345934	0.991392	32.831
DC_case6	1.319188	0.983605	30.212
DC_case7	1.283989	0.972133	26.178
DC_case8	1.236185	0.955429	19.796
DC_case9	1.168207	0.931249	9.205
DC_case10	1.065142	0.897188	0.000
DC_case11	0.892189	0.857587	0.000

Table 7. Comparison of cycle burnup, discharge burnup, and cycle length in EFPMs for a 3-batch refueling scheme for (a) solid cases, (b) dual-cooled annular cases.

(a)

	Cycle burnup (Gwd/t)	Discharge burnup (Gwd/t)	Cycle length (EFPDs)
Reference case	47.479	142.438	685.127
So_case1	56.933	170.800	821.548
So_case2	56.470	169.410	814.863
So_case3	55.671	167.013	803.332
So_case4	54.385	163.154	784.770
So_case5	52.361	157.084	755.573
So_case6	49.187	147.560	709.762
So_case7	44.122	132.365	636.676
So_case8	35.792	107.377	516.484
So_case9	21.724	65.172	313.477
So_case10	1.286	3.858	18.556
So_case11	0.000	0.000	0.000

(b)

	Cycle burnup (Gwd/t)	Discharge burnup (Gwd/t)	Cycle length (EFPDs)
Reference case	47.479	142.438	685.127
DC_case1	55.435	166.306	799.932
DC_case2	54.707	164.121	789.422
DC_case3	53.571	160.714	773.036
DC_case4	53.571	160.714	773.036
DC_case5	49.247	147.740	710.629
DC_case6	45.317	135.952	653.930
DC_case7	39.267	117.802	566.628
DC_case8	29.693	89.080	428.474
DC_case9	13.808	41.423	199.247
DC_case10	0.000	0.000	0.000
DC_case11	0.000	0.000	0.000

3.2. Main actinides tracking

Table 8 presents the atomic densities of the principal actinides from BOC to EOC for all investigated configurations, providing quantitative insight into the isotopic evolution mechanisms that drive the observed burnup performance. All configurations begin with identical initial compositions. The divergent evolution pathways from these common starting

conditions reveal the fundamental neutronic processes governing fuel performance across the spectrum of moderator compositions.

The Th-232 depletion patterns demonstrate a clear correlation with burnup performance and moderator composition. Cases with pure light water moderation exhibit the highest thorium consumption, while consumption progressively decreases as D_2O concentration increases. This variation directly reflects the neutron capture cross-section behavior of thorium, which is strongly enhanced by resonance absorption in the thermal spectrum characteristic of light water. The softer neutron spectrum in H_2O promotes efficient thorium capture, leading to Pa-233 formation, which subsequently decays to fissile U-233. As the spectrum hardens with increasing D_2O content, the resonance integral for thorium capture diminishes, reducing the breeding efficiency. The pure D_2O cases show minimal thorium depletion, confirming that the harder neutron spectrum severely impedes the breeding cycle that is essential for sustaining long-term reactivity in thorium-based fuels.

The fissile isotope evolution reveals complex competing processes that vary dramatically with spectral conditions. U-233 demonstrates particularly interesting behavior, showing net depletion in optimal light water cases despite continuous production from the thorium breeding chain. This indicates that fission rates exceed breeding rates in the thermal spectrum, which is desirable for controlled energy production. Remarkably, in high D_2O cases, U-233 concentrations actually increase substantially above initial values, representing significant accumulation rather than depletion. This counterintuitive increase results from the dramatic reduction in U-233 fission cross-sections in the harder spectrum, which drops by more than two orders of magnitude from thermal to epithermal energies. While breeding continues, albeit at reduced rates, the severely diminished fission probability leads to net accumulation, explaining why these configurations fail to maintain criticality despite building fissile inventory.

U-235 exhibits more predictable depletion patterns across all cases, though consumption rates vary significantly with moderator composition. The highest consumption occurs in pure light water cases where the thermal fission cross-section is maximized, while progressively lower depletion rates are observed with increasing D_2O concentration. The asymmetric depletion behavior between U-233 and U-235 in harder spectra disrupts the intended synergistic operation of the dual-fissile system. The original fuel design assumed balanced consumption of both fissile isotopes to maintain stable reactivity throughout the cycle, but spectral hardening preferentially affects U-233 due to its larger thermal-to-fast cross-section ratio compared to U-235, leading to increasingly imbalanced isotopic vectors that compromise long-term performance.

The protactinium isotope accumulation provides essential insight into breeding dynamics and parasitic absorption pathways. Pa-233, the crucial intermediate in the thorium fuel cycle with a 27-day half-life, reaches equilibrium concentrations that reflect the balance between production from thorium capture and decay to U-233 [47–51]. In optimal light water cases, Pa-233 maintains moderate equilibrium levels indicative of active, efficient breeding where production and decay rates are well-matched. As D_2O concentration increases, Pa-233 concentrations initially remain stable through moderate D_2O additions, then increase significantly in harder spectra. This elevated Pa-233 in high D_2O cases paradoxically indicates less efficient breeding despite higher concentrations, as the longer neutron mean free path and reduced absorption probability in the harder spectrum lead to Pa-233 accumulation rather than efficient conversion through its decay chain. The buildup represents a bottleneck in the breeding process where Pa-233 is produced but not efficiently utilized. Pa-231 accumulation follows a distinctly different pattern, increasing monotonically with D_2O concentration and representing a pure parasitic absorption pathway that removes neutrons from productive reactions. The enhanced Pa-231 production in harder spectra results from alternative neutron

capture chains and reduced fission competition for available neutrons. The nearly doubled Pa-231 burden in pure heavy water cases compared to light water represents a significant additional neutron loss mechanism that further degrades the already compromised neutron economy. This parasitic absorption combines with reduced breeding efficiency to create a compound negative effect on fuel performance in D_2O-moderated systems.

The production of U-232 introduces important backend fuel cycle considerations beyond neutronic performance. This isotope, absent initially, builds up through multiple production pathways, including threshold reactions and complex neutron capture chains. The production rate shows strong spectral dependence, with relatively low generation in pure light water cases where thermal neutrons predominate. Interestingly, U-232 generation does not increase monotonically with D_2O concentration but shows peak production at intermediate concentrations where both threshold reactions and capture processes contribute significantly. The threshold (n,2n) reaction on U-233 requires fast neutrons above approximately 6 MeV, while capture chains through Pa-231 proceed at all energies. The intermediate spectra at moderate D_2O concentrations provide optimal conditions for both mechanisms, maximizing U-232 production. This enhanced generation in mixed moderator systems would necessitate additional radiation protection measures during fuel handling, as U-232's decay chain produces intense gamma radiation, particularly from Tl-208 with its highly penetrating 2.6 MeV gamma rays [49,52–55].

Table 8. Evolution of principal actinide atomic densities in (atoms/b·cm) from BOC to EOC for solid (a) and dual-cooled annular (b) assemblies with varying H_2O/D_2O moderator ratios

(a)

		Th-232	Pa-231	Pa-233	U-232	U-233	U-235
All cases	BOC	2.0596E-02	0.0000E+00	0.0000E+00	0.0000E+00	5.3398E-04	5.2943E-04
So_case1	EOC	1.9913E-02	1.7312E-06	1.5585E-05	1.4737E-06	3.7707E-04	1.2189E-04
So_case2	EOC	1.9900E-02	1.7256E-06	1.5690E-05	1.4875E-06	3.8410E-04	1.2566E-04
So_case3	EOC	1.9885E-02	1.7226E-06	1.5827E-05	1.5019E-06	3.9285E-04	1.3013E-04
So_case4	EOC	1.9866E-02	1.7235E-06	1.6006E-05	1.5169E-06	4.0382E-04	1.3544E-04
So_case5	EOC	1.9842E-02	1.7316E-06	1.6250E-05	1.5320E-06	4.1815E-04	1.4190E-04
So_case6	EOC	1.9811E-02	1.7514E-06	1.6587E-05	1.5458E-06	4.3736E-04	1.4981E-04
So_case7	EOC	1.9769E-02	1.7922E-06	1.7080E-05	1.5556E-06	4.6459E-04	1.5965E-04
So_case8	EOC	1.9709E-02	1.8727E-06	1.7842E-05	1.5555E-06	5.0577E-04	1.7199E-04
So_case9	EOC	1.9617E-02	2.0347E-06	1.9086E-05	1.5314E-06	5.7403E-04	1.8731E-04
So_case10	EOC	1.9464E-02	2.3754E-06	2.1222E-05	1.4497E-06	7.0003E-04	2.0469E-04
So_case11	EOC	1.9175E-02	3.1136E-06	2.4929E-05	1.2462E-06	9.7070E-04	2.1918E-04

(b)

		Th-232	Pa-231	Pa-233	U-232	U-233	U-235
All cases	BOC	2.0596E-02	0.0000E+00	0.0000E+00	0.0000E+00	5.3398E-04	5.2943E-04
DC_case1	EOC	1.9890E-02	1.6219E-06	1.5829E-05	1.3387E-06	3.9637E-04	1.2646E-04
DC_case2	EOC	1.9877E-02	1.6182E-06	1.5950E-05	1.3523E-06	4.0402E-04	1.3037E-04
DC_case3	EOC	1.9860E-02	1.6168E-06	1.6104E-05	1.3666E-06	4.1337E-04	1.3497E-04
DC_case4	EOC	1.9841E-02	1.6193E-06	1.6303E-05	1.3815E-06	4.2506E-04	1.4041E-04
DC_case5	EOC	1.9816E-02	1.6285E-06	1.6568E-05	1.3966E-06	4.4017E-04	1.4698E-04
DC_case6	EOC	1.9784E-02	1.6489E-06	1.6936E-05	1.4106E-06	4.6037E-04	1.5501E-04
DC_case7	EOC	1.9740E-02	1.6893E-06	1.7463E-05	1.4210E-06	4.8878E-04	1.6495E-04
DC_case8	EOC	1.9679E-02	1.7672E-06	1.8261E-05	1.4220E-06	5.3152E-04	1.7733E-04
DC_case9	EOC	1.9586E-02	1.9215E-06	1.9543E-05	1.4007E-06	6.0181E-04	1.9251E-04

DC_case10	EOC	1.9430E-02	2.2439E-06	2.1728E-05	1.3262E-06	7.3165E-04	2.0952E-04
DC_case11	EOC	1.9138E-02	2.9302E-06	2.5408E-05	1.1423E-06	1.0061E-03	2.2294E-04

3.3. Reactivity coefficients

The reactivity coefficient analysis reveals fundamental safety characteristics that demonstrate how the innovative (Th-^{233}U-^{235}U)O_2 fuel responds to operational perturbations under varying moderator compositions and geometric configurations, as illustrated in Figs. 4 and 5. The FTC and MTC serve as fundamental safety parameters governing reactor stability and transient response. The reference UO_2 assembly exhibits FTC of -1.72 pcm/K and MTC of -39.58 pcm/K, establishing conventional baseline values.

The FTC exhibits a systematic progression toward increasingly negative values as deuterium concentration increases, ranging from -2.01 pcm/K for So_case1 with pure H_2O to -10.09 pcm/K for So_case11 with pure D_2O in solid configurations, while dual-cooled annular cases demonstrate even more negative values spanning from -2.32 pcm/K to -10.85 pcm/K across the same compositional range, as depicted in Fig. 4. This enhanced negative feedback stems from the pronounced Doppler broadening effects inherent in thorium-based fuel systems, where the extensive resonance structure of Th-232 in the epithermal energy range becomes increasingly important as the neutron spectrum hardens with rising D_2O content. The thorium resonances provide strong negative reactivity feedback during temperature increases, as broadened absorption peaks capture more neutrons and reduce multiplication, with this effect being amplified in annular geometries due to their altered flux distributions that create more pronounced spectral hardening.

The MTC demonstrates contrasting behavior that transitions from negative to positive values as deuterium concentration increases, presenting critical implications for reactor stability and control characteristics, as shown in Fig. 5. In pure light water configurations, both solid and annular cases maintain strongly negative MTC values of -20.90 and -23.63 pcm/K respectively, providing excellent inherent stability through increased neutron absorption as moderator temperature rises. However, this beneficial negative feedback progressively diminishes with increasing D_2O content, eventually becoming positive at high deuterium concentrations, with So_case11 and DC_case11 exhibiting positive MTC values of +9.71 and +10.46 pcm/K, respectively. This transition occurs because heavy water's exceptional neutron economy and minimal parasitic absorption create conditions where temperature-induced spectral changes and density reductions actually enhance neutron multiplication rather than providing negative feedback. The positive MTC in high D_2O cases represents a significant safety concern, as temperature increases would lead to reactivity increases rather than the desired negative feedback, necessitating enhanced engineered safety systems and more sophisticated control strategies to maintain stable reactor operation under all anticipated operational conditions.

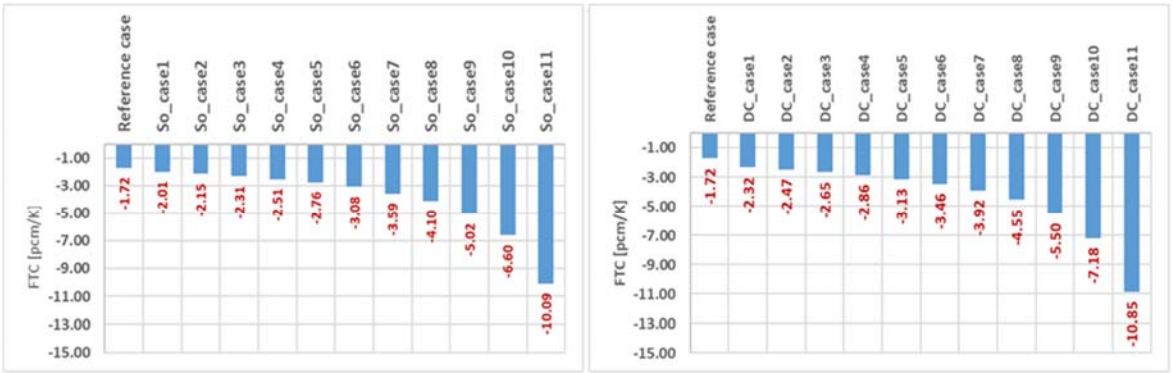

Solid cases **Dual-cooled annular cases**

Figure 4. Comparison of the FTC for the investigated cases.

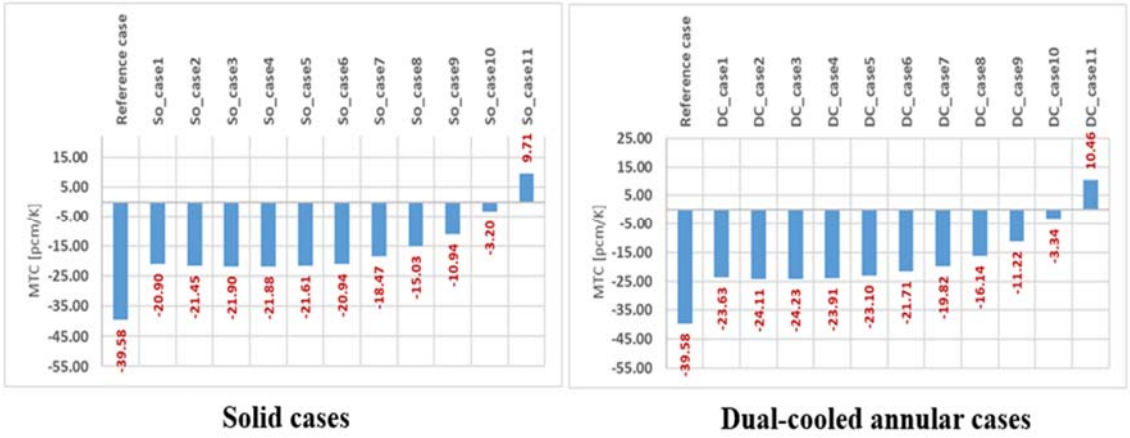

Fig. 5. Comparison of the FTC for the investigated cases.

4. Conclusion and future work

This comprehensive investigation has systematically evaluated mixed H_2O/D_2O moderated reactor assemblies utilizing innovative (Th-^{233}U-^{235}U)O_2 fuel in solid and dual-cooled annular configurations within SMR reactor. The research reveals optimal neutronic performance within the 0-30% D_2O concentration range, where the (Th-^{233}U-^{235}U)O_2 fuel achieves remarkable 20-25% burnup extensions compared to conventional UO_2 fuel. The solid configuration with pure H_2O moderation achieves 170.800 GWd/t discharge burnup and 821.548 EFPD cycle length, while the annular design reaches 166.306 GWd/t and 799.932 EFPDs, approaching targeted 36-month refueling intervals. Superior performance in light water-dominated compositions stems from enhanced thorium utilization and efficient U-233 breeding through Pa-233 decay pathways in the thermal neutron spectrum. Progressive deuterium enrichment beyond 30% causes systematic performance degradation due to spectral hardening that disrupts neutronic balance. Critical safety implications emerge from reactivity coefficient analysis, where fuel temperature coefficients become increasingly negative while moderator temperature coefficients transition from beneficial negative to concerning positive values in heavy water, eliminating essential negative feedback mechanisms.

Future research will address spatial power distribution effects, comprehensive fuel performance analyses including fission gas release and pellet-clad interaction, and nuclear data uncertainties for mixed coolant compositions to provide essential design confidence bounds for practical implementation.

Conflict of interest

There is no conflict of interest in this study.

References

[1] Lloyd C A, Roulstone T and Lyons R E 2021 Transport, constructability, and economic advantages of SMR modularization *Prog. Nucl. Energy* **134** 103672

[2] Carelli M D and Ingersoll D T 2015 *Woodhead Publishing Series in Energy: Number 64 Handbook of Small Modular Nuclear Reactors* ed Elsevier (Woodhead Publishing)

[3] IAEA 2006 *Status of Innovative Small and Medium Sized Reactor Designs 2005*

[4] Zaidabadi Nejad M and Ansarifar G R 2020 Design of a Small Modular Nuclear Reactor with dual cooled annular fuel and investigation of the fuel inner radius effect on the power peaking factor and natural circulation parameters *Ann. Nucl. Energy* **138** 107185

[5] Nejad M Z and Ansarifar G R 2020 Optimal design of a Small Modular Reactor core with dual cooled annular fuel based on the neutronics and natural circulation parameters *Nucl. Eng. Des.* **360** 110518

[6] Zhang Z, Wu T, Wang Y, Chen S, Yuan C and Zhu J 2021 Core design and neutronic study on small reactor with advanced fuel designs *Nucl. Mater. Energy* **29** 101068

[7] Deng Y, Qiu B, Yin Y, Wu Y and Su G 2022 Investigation on fuel cracking induced relocation behavior of dual-cooled annular fuel based on finite element simulation *J. Nucl. Mater.* **567** 153779

[8] Liu S, Liu R and Qiu C 2022 CAMPUS-ANNULAR: Preliminary multiphysics modeling of annular fuel performance under normal operating and accident conditions *Prog. Nucl. Energy* **153** 104430

[9] Xu Z, Otsuka Y, Hejzlar P, Kazimi M S and Driscoll M J 2007 High-performance annular fuel reactor physics and fuel management *Nucl. Technol.* **160** 63–79

[10] Kazimi M S and Hejzlar P 2006 *High Performance Fuel Design for Next Generation PWRs: Final Report*

[11] Hejzlar P and Kazimi M S 2007 Annular fuel for high-power-density pressurized water reactors: Motivation and overview *Nucl. Technol.* **160** 2–15

[12] Zhiwen Xu 2003 *Design Strategies for Optimization High Burn-up Fuel in Pressurized Water Reactor Reactors* (Massachusetts Institute of Technology)

[13] Hassan I A, Badawi A A, El Saghir A and Shaat M K 2019 Viability of uranium nitride (UN) as annular fuel for AP-1000 *Prog. Nucl. Energy* **110** 170–7

[14] Shin C H, Chun T H, Oh D S and In W K 2012 Thermal hydraulic performance assessment of dual-cooled annular nuclear fuel for OPR-1000 *Nucl. Eng. Des.* **243** 291–300

[15] Feng D, Hejzlar P and Kazimi M S 2007 Thermal-Hydraulic Design of High-Power-Density Annular Fuel in PWRs *Nucl. Technol.* **160** 16–44

[16] Kazimi M S 2007 Introduction to the annular fuel special issue *Nucl. Technol.* **160** 1

[17] Kabach O, Mahjoub Chakir E and Amsil H 2024 Innovative burnable absorbers: Assessing PaO2 and NpO2 coatings for improved safety in (Th-233U-235U)O2 fuel assemblies *Nucl. Eng. Des.* **421** 113086

[18] Bouassa T, Kabach O and Chakir E M 2024 Neutronic analysis of different sandwich cladding material options for (Th-233U-235U)O2 annular fuel in advanced PWR assembly *Interactions* **245** 239

[19] Lkouz M, Kabach O, Chetaine A, Saidi A and Bouassa T 2023 Revolutionizing LWR SMR reactors: exploring the potential of (Th- 233 U- 235 U)O 2 fuel through a parametric study *Energy Sources, Part A Recover. Util. Environ. Eff.* **45** 10162–75

[20] Bouassa T, Kabach O, Chetaine A, Benrhnia Z, El Banni F and Saidi A 2023 Parametric

neutronic analysis of different cladding options for ThO2 pellet of advanced dual-cooled annular PWR assembly *Nucl. Eng. Des.* **414** 112533

[21] Lkouz M, Kabach O and Chetaine A 2023 Enhancing temperature reactivity coefficients in SMR Reactor with (Th233U- 235U) 2 fuel through PaO2 as a burnable absorber *Ann. Univ. Craiova, Phys.* **33** 181–90

[22] Benrhnia Z, Kabach O, Chetaine A and Saidi A 2022 Analysis of reactivity control coefficients and the stability of an AP1000 reactor assembly fueled with (Th- 233 U)O2 using DRAGON code *Ann. Univ. Craiova, Phys.* **32** 88–102

[23] Benrhnia Z, Chetaine A, Kabach O, Amsil H, Benchrif A and El Banni F 2022 Neutronic and burnup characteristics of potential dual- cooled annular (Th-233U-235U)O2 fuel for the advanced pressurized water reactors: An assembly-level analysis *Int. J. Energy Res.* **46** 23501–16

[24] El Banni F, Gogon B L H, Kabach O and Chakir E M 2024 Analyzing (Th-233U-235U)O2 fuel performance in various assembly configurations: A comparative neutronic study *Nucl. Energy Technol.* **10** 169–78

[25] Rifai H, Kabach O, Sadoune Z, Chakir E M, Uzun S, Amsil H and Banni F El 2025 Innovative thorium-based fuel assemblies for LW-SMR: In-depth assembly-level neutronic analysis and safety considerations in solid and annular configurations *Nucl. Eng. Des.* **442** 114274

[26] DOE 2010 *Fuel Cycle Analysis of Once-Through Nuclear Systems*

[27] Stacey W M 2007 *Nuclear Reactor Physics: Second Edition*

[28] Lewis E E 2008 Neutron Interactions *Fundamentals of Nuclear Reactor Physics* (Elsevier) pp 29–56

[29] Rahimi G, Hadad K, Nematollahi M, Zarifi E and Sahin S 2020 Comparison of semi-heavy water and H2O as coolant for a conceptual research reactor from the view point of neutronic parameters *Prog. Nucl. Energy* **118** 103126

[30] Alam S B, Goodwin C S and Parks G T 2019 Parametric neutronics analyses of lattice geometry and coolant candidates for a soluble-boron-free civil marine SMR core using micro-heterogeneous duplex fuel *Ann. Nucl. Energy* **129** 1–12

[31] Vempalle A 2023 Assessing Criteria to Pick Ideal Moderators for Nuclear Fission Reactors *J. Student Res.* **12** 1–7

[32] Westinghouse Electric Company LLC 2004 *Chapter 4.3 Nuclear Design AP1000 DCD*

[33] Laranjo de Stefani G, Losada Moreira J M, Maiorino J R and Russo Rossi P C 2019 Detailed neutronic calculations of the AP1000 reactor core with the Serpent code *Prog. Nucl. Energy* **116** 95–107

[34] Schulz T L 2006 Westinghouse AP1000 advanced passive plant *Nucl. Eng. Des.* **236** 1547–57

[35] IAEA 2024 *SMALL MODULAR REACTOR TECHNOLOGY CATALOGUE*

[36] Westinghouse Electric Company LLC 2023 AP300TM Small Modular Reactor

[37] IAEA 2008 *Thermophysical Properties of Materials For Nuclear Engineering: A Tutorial and Collection of Data*

[38] Herring J S and MacDonald P E 1999 *Characteristics of mixed Thorium – Uranium dioxide high burnup fuel*

[39] Marleau G, Hebert A, Roy R and Hébert A 2021 *A USER GUIDE FOR DRAGON VERSION5*

[40] Paradis M, Doligez X, Marleau G, Ernoult M and Thiollière N 2022 DONJON5/CLASS coupled simulations of MOX/UO 2 heterogeneous PWR core *EPJ Nucl. Sci. Technol.* **8** 4

[41] El Kheiri O, Kabach O, Chetaine A and Abdelmajid S 2023 Application of high-thickness integral fuel burnable absorber ZrB2 in a dual-cooled micro-heterogeneous duplex fuel for small modular long-life reactor *Ann. Univ. Craiova, Phys.* **33** 171–80

[42] Radi A, Kabach O and Chakir E M 2024 Calculations of the principal neutronic characteristics of a hypothetical VVER assembly with minor actinides incorporated into PuO2-ThO2 fuel in a duplex configuration *Nucl. Energy Technol.* **10** 221–33

[43] El Kheiri O, Kabach O and Chetaine A 2023 Neutronic investigation of prospective dual-cooled micro-heterogeneous duplex fuel for small modular long-life reactors: Assembly level design and analysis *Prog. Nucl. Energy* **160** 104680

[44] Driscoll M J, Downar T J and Pilat E E 1991 *The Linear Reactivity Model For Nuclear Fuel Management* (American Nuclear Society)

[45] Burns J R, Hernandez R, Terrani K A, Nelson A T and Brown N R 2020 Reactor and fuel cycle performance of light water reactor fuel with 235U enrichments above 5% *Ann. Nucl. Energy* **142** 107423

[46] Hernandez R and Brown N R 2020 Potential fuel cycle performance of floating small modular light water reactors of Russian origin *Ann. Nucl. Energy* **144** 107555

[47] Kabach O 2021 *Possible Scenarios for a Transition to a Thorium-Based Fuel Cycle in a Pebble-Bed High-Temperature Reactor* (Mohammed V University in Rabat)

[48] DEMERS Z 2017 *Comparative Safety Evaluation of Thorium Fuel to Natural Uranium Fuel in a CANDU 6 Reactor* (McMaster University)

[49] Insulander Björk K 2015 *Thorium Fuels for Light Water Reactors Steps towards commercialization* (Chalmers University of Technology)

[50] Baldová D 2014 *Feasibility study on high-conversion Th-U233 fuel cycle for current generation of PWRs* (Czech Technical University in Prague)

[51] Zohuri B 2019 *Neutronic Analysis For Nuclear Reactor Systems* (Cham: Springer International Publishing)

[52] Volaski D 2010 *Investigation of Breeding Potential of U233-Th Cycle in Light Water Reactors* (BEN-GURION UNIVERSITY OF THE NEGEV)

[53] Insulander Björk K and Netterbrant C 2018 Thorium as an additive for improved neutronic properties in boiling water reactor fuel *Ann. Nucl. Energy* **113** 470–5

[54] Kang J and von Hippel F N 2001 U-232 and the proliferation-resistance of U-233 in spent fuel *Sci. Glob. Secur.* **9** 1–32

[55] Nuclear Energy Agency 2015 *Introduction of thorium in the nuclear fuel cycle* vol 1